cmgh
CELLULAR AND MOLECULAR GASTROENTEROLOGY AND HEPATOLOGY

ORIGINAL RESEARCH

The Glucocorticoid Receptor in Intestinal Epithelial Cells Alleviates Colitis and Associated Colorectal Cancer in Mice

Chiara Muzzi,[1,*] Norika Watanabe,[1,*] Eric Twomey,[1,*] Garrit K. Meers,[1] Holger M. Reichardt,[1] Hanibal Bohnenberger,[2] and Sybille D. Reichardt[1]

[1]*Institute for Cellular and Molecular Immunology, University Medical Center Göttingen, Göttingen, Germany; and* [2]*Institute of Pathology, University Medical Center Göttingen, Göttingen, Germany*

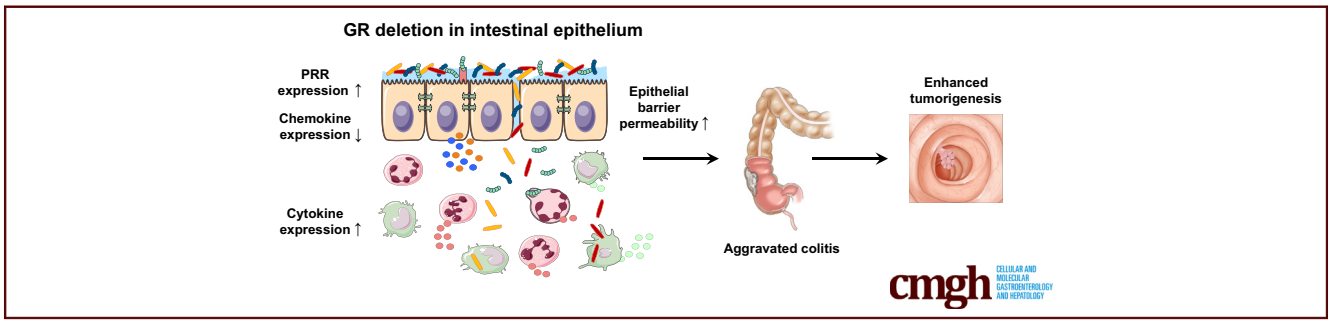

SUMMARY

The glucocorticoid receptor in intestinal epithelial cells plays a crucial role in colonic inflammation by regulating gene expression, leukocyte recruitment, and epithelial barrier permeability, and thereby indirectly impacts tumorigenesis in the colon.

BACKGROUND & AIMS: Inflammatory bowel disease is commonly treated by administration of glucocorticoids. While the importance of intestinal epithelial cells for the pathogenesis of this disorder is widely accepted, their role as target cells for glucocorticoids has not been explored. To address this issue, we induced colonic inflammation in GR^{villin} mice, which carry an inducible deletion of the glucocorticoid receptor in intestinal epithelial cells.

METHODS: Colitis and colitis-associated colorectal cancer were induced by administration of dextran sulfate sodium and azoxymethane in mice. Clinical parameters, epithelial permeability and tumor development were monitored during disease progression. Colon tissue, lamina propria cells and intestinal epithelial cells were examined by gene expression analyses, flow cytometry, histopathology, and immunohistochemistry.

RESULTS: The absence of the intestinal epithelial glucocorticoid receptor aggravated clinical symptoms and tissue damage, and compromised epithelial barrier integrity during colitis. Gene expression of chemokines, pattern recognition receptors and molecules controlling epithelial permeability was dysregulated in intestinal epithelial cells of GR^{villin} mice, leading to a reduced recruitment and a hyperactivation of leukocytes in the lamina propria of the colon. Importantly, the exaggerated inflammatory response in GR^{villin} mice also enhanced associated tumorigenesis, resulting in a higher number and larger size of tumors in the colon.

CONCLUSIONS: Our results reveal an important role of intestinal epithelial cells as targets of glucocorticoid action in inflammatory bowel disease and suggest that the efficacy with which colitis is kept at bay directly affects the progression of colorectal cancer. *(Cell Mol Gastroenterol Hepatol 2021;11:1505–1518; https://doi.org/10.1016/j.jcmgh.2020.12.006)*

Keywords: Colon; Inflammation; Tumor; Epithelial Barrier.

*Authors share co-first authorship.

Abbreviations used in this paper: **AOM, azoxymethane; CA-CRC, colitis-associated colorectal cancer; DSS, dextran sulfate sodium; DAI, disease activity index; EB, Evan's blue; GC, glucocorticoid; GR, glucocorticoid receptor; IBD, inflammatory bowel disease; IEC, intestinal epithelial cell; IL, interleukin; LPC, lamina propria cell; mRNA, messenger RNA; NF-κB, nuclear factor kappa B; PBS, phosphate-buffered saline; RT-PCR, reversetranscription polymerase chain reaction; TNF-α, tumor necrosis factor α; TNFR2, tumor necrosis factor receptor 2; UC, ulcerative colitis.**

Most current article

2352-345X
https://doi.org/10.1016/j.jcmgh.2020.12.006

The luminal surface of the gut is the largest area of the body that is in constant contact with the outer environment. As a first line of protection, intestinal epithelial cells (IECs) prevent the invasion of potentially harmful microorganisms. Disruption of the epithelial barrier not only causes infections but can also lead to chronic intestinal inflammation, which is commonly referred to as inflammatory bowel disease (IBD). There are 2 major forms of IBD, namely ulcerative colitis (UC) and Crohn's disease, which share many clinical symptoms such as abdominal pain, weight loss, diarrhea, and rectal bleeding.[1] UC is the more common form of IBD, also occurs in younger individuals, and represents a major risk factor for the development of colitis-associated colorectal cancer (CA-CRC), one of the most frequent tumor entities worldwide.[2–4]

Currently, there is no cure for IBD. Although treatment with monoclonal antibodies targeting tumor necrosis factor α (TNF-α) and VLA-4 (very late antigen 4) provided promising results, glucocorticoids (GCs) remain the mainstay in IBD therapy.[5,6] Patients suffering from severe symptoms or experiencing an acute relapse commonly receive high doses of GCs. Once remission is achieved, the dose is tampered, which is important because prolonged administration of GCs is accompanied by adverse effects such as diabetes, osteoporosis, and hypertension.[7] These complications arise when the drug binds to the ubiquitously expressed GC receptor (GR) in cell types involved in a variety of physiological processes. Hence, a better understanding of the mode of GC action in the treatment of IBD might help to develop better therapeutic strategies.

Considerable efforts have been made to unveil the mechanisms of GCs in controlling clinical symptoms of UC, frequently using the colitis mouse model induced by dextran sulfate sodium (DSS). Our own work for instance revealed the importance of GC activities in macrophages and neutrophils in this disease. We could show that GR deletion in myeloid cells compromised the resolution of the inflammatory response in DSS-induced colitis, whereas the acute phase was unaffected.[8] More specifically, macrophage infiltration into the inflamed colon as well as their polarization was altered. Several other publications also reported on attempts to treat DSS-induced colitis in rodent models with GCs, albeit such an approach provided inconsistent results. In contrast to the beneficial effects of GCs in IBD patients, dexamethasone treatment of acute colitis aggravated clinical symptoms rather than ameliorating them, a phenomenon which is not yet understood.[9–11] Based on this observation, the analysis of GR knockout mice currently appears to be the preferred strategy to explore GC activities in experimental colitis.

Progress has also been made in understanding the mechanisms that underlie the disruption of intestinal homeostasis in IBD. Prominent participants in this process are IECs, the resident and infiltrating immune cells in the lamina propria, as well as the microbiota. IECs serve as a communication interface between these 3 components. On the one hand, they are able to detect and recognize potentially harmful microorganisms, and on the other hand, they transmit and receive signals to and from immune cells that reside in the lamina propria.[12,13] Thus, IECs are ideally positioned to function as a rheostat of mucosal gut immunity.

There is a long-established relationship between a dysfunctional intestinal epithelium and IBD. Several studies supported an association between an increased intestinal permeability and the inflammatory response in the acute phase of the disease.[14–16] Only very little information, however, is available as to the role of GC activities in IECs in humans and mice. One recent publication reported that proinflammatory cytokines and chemokines were transiently upregulated after selective deletion of the intestinal epithelial GR, but whether these moderate effects impact the severity of colitis remained unknown.[17] Whereas IECs are undoubtedly important players in the pathogenesis of IBD, their role as targets of GC activity has thus not yet been explored in detail.

UC is a major risk factor for the development of CRC in young individuals.[18] Inflammation in the colon initiates multiple events such as the secretion of cytokines and reactive oxygen species that are aimed at the elimination of pathogens and tissue repair. However, these mediators can also induce gene mutations, in particular in IECs, and thereby foster tumorigenesis. There are a number of signaling pathways involved in the development of CA-CRC. For example, the nuclear factor kappa B (NF-κB) pathway is crucial in the context of inflammation and also promotes the proliferation and survival of tumor cells.[19] Experimental evidence that this pathway is involved in CA-CRC was obtained by using IKKβ knockout mice.[20] In a mouse model of CA-CRC induced by the combined administration of azoxymethane (AOM) and DSS it could be shown that the tumor incidence was significantly reduced when established in mice selectively lacking IKKβ in IECs. Furthermore, it was found that serum levels of interleukin (IL)-6, which is synthesized in an NF-κB–dependent manner, correlated with the stage and size of tumors in human CRC.[21] Prostaglandin synthesis is also associated with tumorigenesis as it could be shown that tumor burden was reduced in COX-2 (cyclooxygenase-2) knockout mice tested in a genetic model of CRC.[22] In addition, studies in mice and humans indicate a protective role of the COX-2 inhibitor aspirin for the development of CRC.[23,24] Overall, there is a plethora of evidence that inflammatory pathways impact CRC, suggesting that there could be a correlation between the anti-inflammatory activity of GCs in the colon and tumorigenesis as well.

In this work, we investigated the impact of GC activities in IECs by using 2 models of UC and CA-CRC established in mice carrying an inducible deletion of the intestinal epithelial GR. Our finding that the severity of DSS-induced colitis was enhanced in mutant mice and that this had a direct impact on tumor burden in the AOM/DSS model warrants efforts to further optimize GC therapy of IBD, for instance by targeted delivery of these drugs to IECs.

Results

GR Deletion in IECs Aggravates DSS-Induced Colitis

GR^{villin} mice carrying an inducible deletion of the GR in IECs were employed to investigate the role of GCs in the

colon using mouse models of UC and CA-CRC. Gene recombination was induced by oral administration of tamoxifen and selectively occurred in the jejunum, ileum, and colon but not in the stomach of GR^{villin} mice (Figure 1*A*). No recombination of the GR locus was observed in GR^{flox} mice. The epithelial lining in the colon of GR^{villin} mice was devoid of any GR immunoreactivity, whereas cells in the lamina propria and tunica muscularis still expressed the GR (Figure 1*B*). In GR^{flox} mice, the GR was present in all cells of the colon.

DSS-treatment of GR^{villin} and GR^{flox} mice resulted in a progressive reduction in body weight, an effect that was exaggerated in the absence of the GR in IECs (Figure 1*C* and *D*). The disease activity index (DAI) score, which combines 3 major clinical hallmarks of colitis, started to rise shortly after the onset of DSS treatment, was aggravated until day 10, and was higher in GR^{villin} than GR^{flox} mice (Figure 1*E*). The body weight and DAI score of control mice remained unaltered regardless of the genotype (Figure 1*D* and *E*). The length of the colon at day 10 was reduced in GR^{villin} compared with GR^{flox} mice, whereas IL-6 serum levels were increased (Figure 1*F* and *G*). These data collectively suggest that GR deletion in IECs exacerbates experimentally induced colitis in mice.

Increased Tissue Damage and Epithelial Permeability in GR^{villin} Mice

DSS-treatment causes extensive tissue destruction in the colon. Evaluation of histological sections collected at day 10 revealed enhanced tissue damage in GR^{villin} compared with GR^{flox} mice as reflected by the increased histological score, whereas no abnormalities were seen in control mice (Figure 2*A* and *B*). Because DSS treatment compromises epithelial barrier integrity as well, we assessed its permeability with an assay in which the amount of Evan's blue (EB) dye is quantified that diffuses from the lumen of the colon into the tissue. As expected, mice suffering from DSS-induced colitis contained more EB in the tissue at day 10 than healthy control mice (Figure 2*C* and *D*). Importantly, EB accumulation in diseased GR^{villin} mice was higher than in GR^{flox} mice, which indicates that the epithelial permeability was enhanced (Figure 2*C* and *D*). We conclude that GR deletion in IECs exacerbates both tissue destruction and the loss of epithelial barrier integrity during DSS-induced colitis.

High-Throughput Gene Expression Analysis of the Inflamed Colon

To obtain a first impression of the gene expression profile in the colon of GR^{villin} mice during DSS-induced colitis, a microfluidic dynamic array platform for high-throughput quantitative reverse transcription polymerase chain reaction (RT-PCR) was employed. Analysis of 12 selected genes in colon biopsies collected from healthy and diseased mice at day 10 revealed 4 distinct expression patterns (Figure 3). Chemokines of the *Cxcl* family were upregulated in GR^{flox} but not GR^{villin} mice during DSS-induced colitis, whereas chemokines of the *Ccl* family were even higher in GR^{villin} compared with GR^{flox} mice. Members of the *Tlr* family were generally more abundant in GR^{villin} than GR^{flox} mice, while the gene encoding ornithine transcarboxylase (*Otc*), which is preferentially expressed by epithelial cells, was downregulated during DSS-induced colitis regardless of the genotype.

Cell-Intrinsic Effects of GR Deletion in IECs

Considering the cell-type specificity of the mutation in GR^{villin} mice, we next investigated gene expression in IECs purified from the colon by quantitative RT-PCR. Expression of *Cxcl1*, *Cxcl5*, and *Ccl5*, 3 chemokines known to play an important role in the pathogenesis of colitis, was upregulated during DSS-induced colitis in GR^{flox} but not in GR^{villin} mice (Figure 4). This finding indicates that the GR is required for full induction of chemokine expression in IECs during inflammation. Some other genes, however, were overexpressed in IECs of GR^{villin} compared with GR^{flox} mice, indicating a loss of repression due to the deletion of the GR. This situation was found for *Tlr4*, which is involved in pathogen sensing, as well as *Tnfr2* and *Mlck*, 2 genes that cooperate in the control of epithelial barrier integrity (Figure 4). Based on these data, we conclude that the GR uses different transcriptional mechanisms to regulate gene expression in IECs.

Reduced Leukocyte Infiltration in GR^{villin} Mice

Chemokines secreted by IECs including CXCL1, CXCL5, and CCL5 play an important role in attracting leukocytes such as neutrophils and monocytes. Hence, we asked whether their reduced expression in IECs of GR^{villin} mice had any impact on the infiltration of myeloid cells during DSS-induced colitis. To address this question, lamina propria cells (LPCs) were isolated from healthy and diseased mice at day 10, and the abundance of different leukocyte subtypes was compared between GR^{villin} and GR^{flox} mice by flow cytometry. Neutrophils were defined as $CD11b^{+}Ly6G^{+}$ cells, while $CD11b^{+}Ly6G^{-}$ cells were considered as macrophages. Inflammatory macrophages were distinguished from resting ones based on their expression of Ly6C (Figure 5). In agreement with the regulation of chemokine expression in IECs, the abundance of neutrophils, total macrophages, and inflammatory macrophages in the lamina propria of GR^{villin} mice was reduced during DSS-induced colitis compared with GR^{flox} mice, whereas no differences were found in control mice (Figure 6*A*). This finding indicates that the recruitment of myeloid cells into the inflamed colon is impaired in the absence of the GR in IECs.

Hyperactivation of Infiltrating Leukocytes in the Colon of GR^{villin} Mice

Despite the lower number of neutrophils and macrophages in the colon of GR^{villin} mice during DSS-induced colitis, clinical and histological hallmarks of colitis were exacerbated in mutant mice. Therefore, we examined the expression of proinflammatory genes in LPCs isolated from the colon. Surprisingly, *Cxcl1*, *Cxcl5*, and *Ccl5* messenger RNA (mRNA) levels in LPCs of GR^{villin} mice were higher than in GR^{flox} mice during DSS-induced colitis (Figure 6*B*). In addition, mRNA levels of *Il1b*, *Il6*, and *Ptgs2 (Cox2)* were also

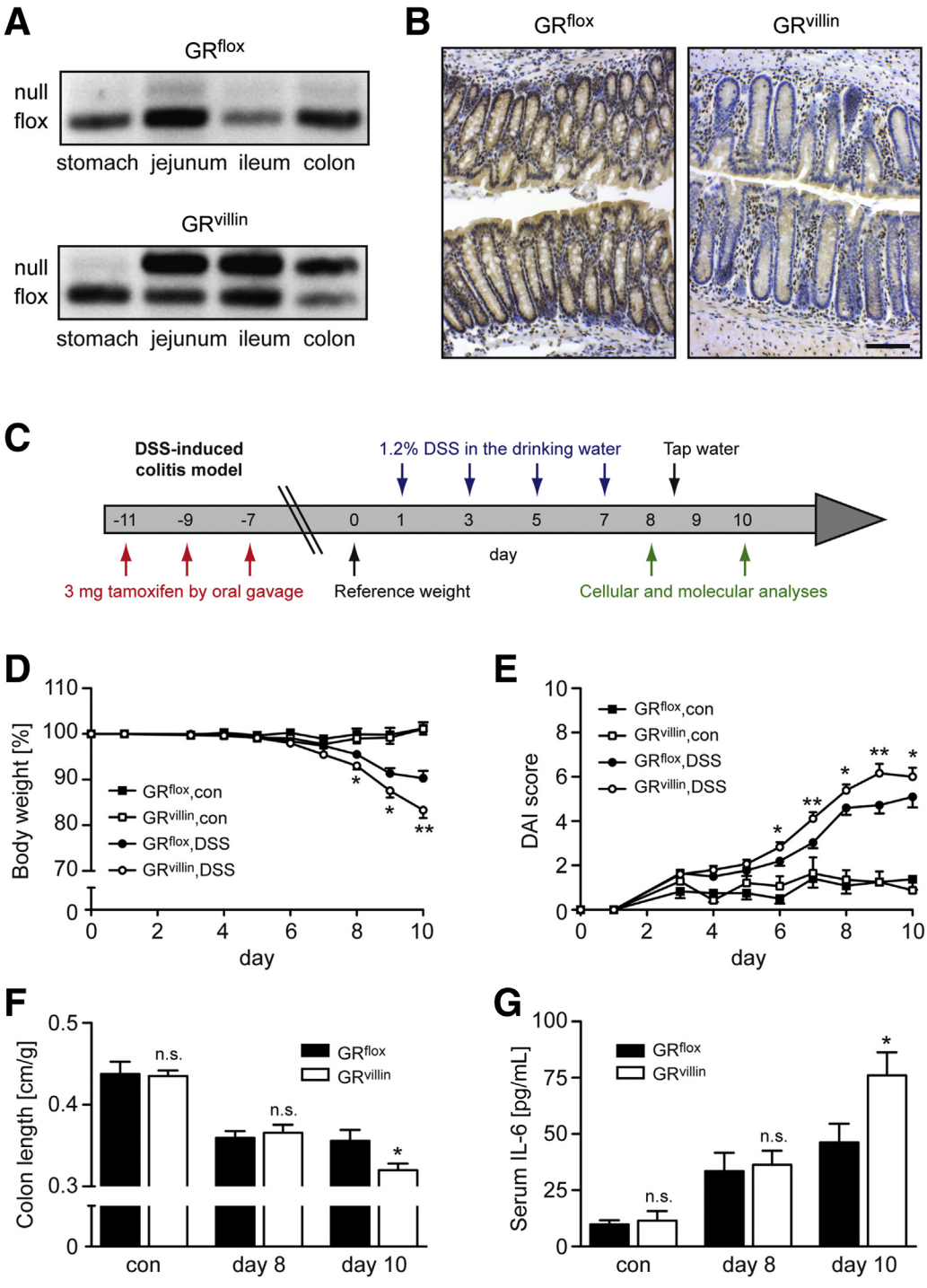

Figure 1. Inducible deletion of the GR in IECs and its impact on DSS-induced colitis. (*A*) GR^{flox} and GR^{villin} mice received tamoxifen over a 5-day period. Three weeks later, genomic DNA was prepared from 4 different regions of the gastrointestinal tract and amplified with primers distinguishing between the unrecombined flox and the recombined null allele of the GR locus. One representative experiment out of 2 is shown. (*B*) Paraffin sections were prepared from the colon of mice treated as in panel *A* and stained with an anti-GR antibody. One representative microphotograph each is depicted at 20× magnification. Scale bar = 200 μm (*C*) Experimental setup of the DSS-induced colitis model. (*D*, *E*) Mice were treated as outlined in panel *C*. Control (con) mice received tap water only. The body weight is depicted relative to the weight measured at day 0, and the DAI score was calculated based on stool consistence, intestinal bleeding, and weight loss. GR^{flox} mice: n = 6/31, GR^{villin} mice: n = 7/39 (con/DSS). (*F*) The colon length of mice sacrificed at day 8 or 10 of DSS treatment or control mice was measured from the ileocecal junction to the rectum and is depicted in relation to the body weight. GR^{flox} mice: n = 4/7/9, GR^{villin} mice: n = 3/9/13 (con/ day 8/day 10). (*G*). IL-6 serum levels of mice sacrificed at day 8 or 10 of DSS treatment or control mice were analyzed by ELISA. GR^{flox} mice: n = 3/3/4, GR^{villin} mice: n = 2/7/6 (con/8/10). All values are depicted as the mean ± SEM. Statistical analysis was performed by 1-way analysis of variance followed by Newman-Keuls Multiple Comparison test. Statistical analysis in panels *D* and *E* was performed individually for each day and is depicted for the comparison of DSS-treated GR^{flox} and GR^{villin} mice. Statistical analysis in panels *C* and *D* was performed for the entire data set and is depicted for the comparison of GR^{flox} and GR^{villin} mice at each time point. Levels of significance: $^{*}P < .05$; $^{**}P < .01$; n.s., nonsignificant ($P > .5$).

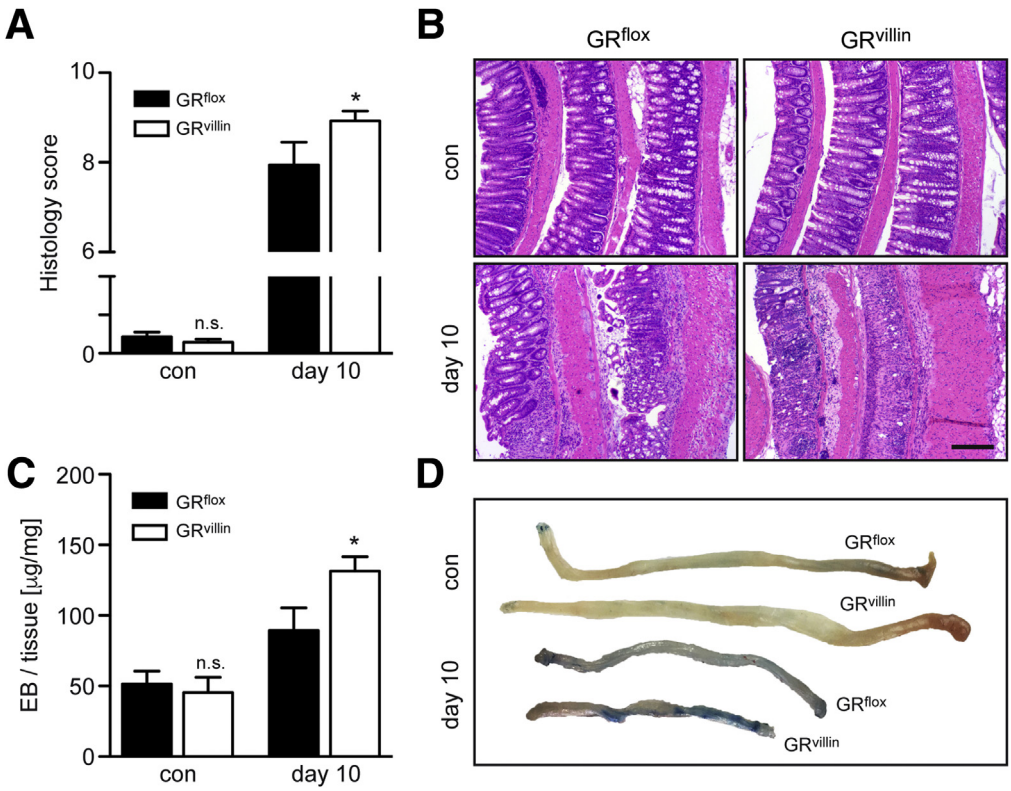

Figure 2. Histological assessment of tissue damage in the colon and analysis of the epithelial barrier integrity in DSS-induced colitis. GR^{flox} and GR^{villin} mice were treated as outlined in Figure 1*C*. Control (con) mice received only tap water. (*A*) Swiss rolls of the colon were prepared from DSS-treated and untreated mice at day 10, and paraffin sections stained with hematoxylin and eosin were evaluated for tissue damage by assessing inflammatory infiltration, crypt distortion, and the loss of goblet cells, which is collectively depicted as a histological score. GR^{flox} mice: n = 6/8, GR^{villin} mice: n = 9/17 (con/day 10). (*B*) Representative photomicrographs of hematoxylin and eosin stained sections of the colon at 10× magnification. Scale bar = 400 μm. (C) The colon was dissected from DSS-treated and control mice at day 10, filled with EB dye solution, and incubated for 1 hour. EB that had diffused into the tissue was extracted after washing and quantified by spectrophotometry to determine epithelial permeability. The amount of EB is depicted in relation to the weight of the colon. GR^{flox} mice: n = 4/7, GR^{villin} mice: n = 3/6 (con/day 10). (*D*) Representative photographs of the colon after incubation with EB. Values in panels *A* and *C* are depicted as the mean ± SEM. Statistical analysis was performed by 1-way analysis of variance followed by Newman-Keuls Multiple Comparison test and is depicted for the comparison of GR^{flox} and GR^{villin} mice at each time point. Levels of significance: *$P < .05$; n.s., nonsignificant ($P > .5$).

overexpressed in LPCs of GR^{villin} mice during DSS-induced colitis (Figure 6*B*). This observation unveils a hyperactivation of LPCs, presumably concerning the infiltrating neutrophils and macrophages. Because the GR is expressed at normal levels in these cells, it is fair to assume that the observed effect is a consequence of the aggravated tissue damage and probably also the increased microbial invasion in GR^{villin} mice.

Enhanced Tumorigenesis in the Colon of GR^{villin} Mice

Colitis is an important risk factor for the development of CRC. Therefore, we asked whether the enhanced severity of DSS-induced colitis in GR^{villin} mice had any impact on tumorigenesis initiated by the carcinogenic agent AOM. Mice in which the GR had been selectively deleted in IECs were treated with DSS to elicit colitis as well as with AOM to initiate tumor development (Figure 7*A*). Similar to our earlier finding, DSS-induced colitis in GR^{villin} mice was significantly more severe than in GR^{flox} mice as indicated by the higher DAI score (Figure 7*B*). Starting in week 7, tumorigenesis was monitored by colonoscopy until tumors of stage S3 had developed (Figure 8). Macroscopic inspection in week 9 revealed that most tumors were localized at the rectal part of the colon (Figure 7*C*). Histological analysis demonstrated a diffuse epithelial morphology of the tumors and confirmed that the GR was absent from these epithelial-like cells (Figure 7*D*). Most importantly, the average number of tumors in GR^{villin} mice was significantly higher than in GR^{flox} mice, and their size was increased as well (Figure 7*E*). Consequently, the overall tumor burden in GR^{villin} mice was more than twice as large as in GR^{flox} mice (Figure 7*E*). Interestingly, the abundance of $CD3^+$ T cells and $CD68^+$ myeloid cells in GR^{villin} and GR^{flox} mice was similar, both in the tumor itself and in the adjacent mucosal tissue (Figure 9*A* and *B*). The enhanced tumorigenesis in GR^{villin} mice therefore seems to be unrelated to differences in leukocyte infiltration.

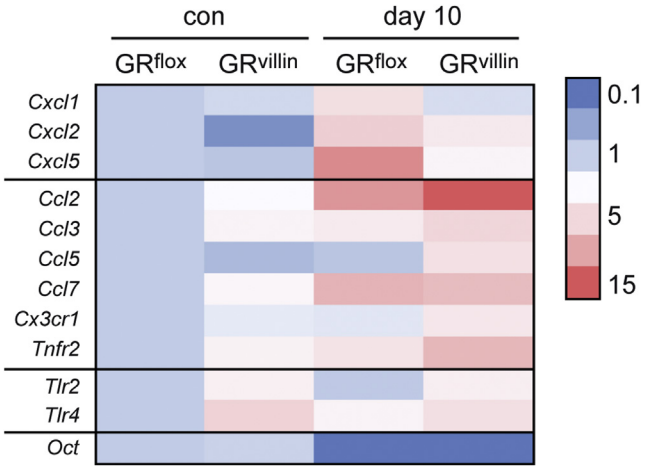

Figure 3. Gene expression analysis of the colon in DSS-induced colitis using high-throughput quantitative RT-PCR. GR^{flox} and GR^{villin} mice were treated with tamoxifen to initiate GR deletion in IECs and subsequently received DSS to induce colitis. Control (con) mice received only tap water. The colon was dissected from mice sacrificed at day 10 of DSS treatment or untreated mice and total RNA was isolated from the entire organ. Gene expression analysis was done using a microfluidic dynamic array platform. Differences in gene expression are visualized using a color code, with the lowest expression depicted in blue and the highest expression in red. Gene expression of untreated (con) GR^{flox} mice was arbitrarily set to 1. Genes were grouped based on their different patterns of regulation.

Tumor Progression Is Linked to the Severity of DSS-Induced Colitis

The increased tumor burden in GR^{villin} mice could be related to the aggravated colitis or directly caused by the absence of the GR in IECs. To distinguish between these 2 possibilities, we induced colitis by DSS treatment before the GR was deleted in IECs (Figure 10*A*). As expected, the severity of clinical symptoms based on the DAI score was similar in mice of both genotypes, which is consistent with the unaltered GR expression in IECs under these conditions (Figure 10*B*). Once the disease had started to resolve, the GR was deleted by tamoxifen administration and tumorigenesis was monitored by colonoscopy until week 9. Macroscopic inspection of the colon revealed a comparable number and similar area of tumors in GR^{villin} and GR^{flox} mice in this experimental setting (Figure 10*C*). Hence, there was also no difference in the overall tumor burden between genotypes (Figure 10*C*). This observation confirms that tumorigenesis is directly linked to the severity of colitis rather than being related to the presence of the GR in IECs.

Discussion

Synthetic GCs such as prednisolone are widely used to treat UC despite being complicated by the occurrence of steroid resistance and various side effects.[6] In principle, GCs can act on any cell type in the colon including resident and infiltrating leukocytes as well as IECs. Previous work from

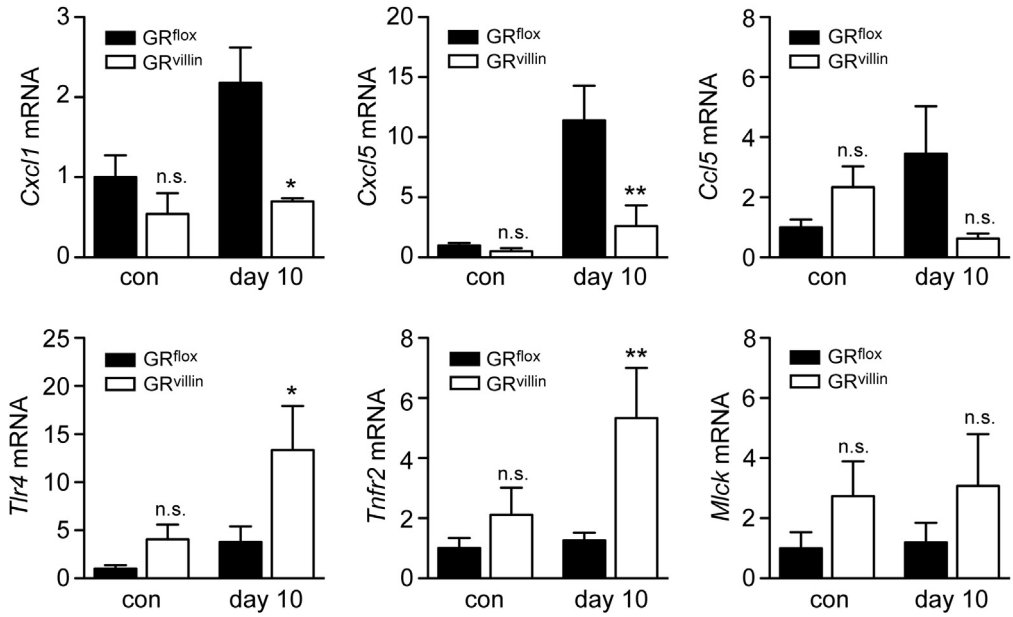

Figure 4. Gene expression analysis of IECs prepared from the colon in DSS-induced colitis. GR^{flox} and GR^{villin} mice were treated with tamoxifen to initiate GR deletion in IECs and subsequently received DSS to induce colitis. Control (con) mice received only tap water. IECs were prepared from the colon of DSS-treated mice at day 10 or control mice, and gene expression was analyzed by quantitative RT-PCR. Relative mRNA levels of *Cxcl1*, *Cxcl2*, and *Ccl5* as well as *Tlr4*, *Tnfr2*, and *Mlck* were determined by normalization to the housekeeping gene *Hprt*. Expression levels in untreated (con) GR^{flox} mice were arbitrarily set to 1. GR^{flox}, con: n = 5–6, GR^{flox}, DSS: n = 6–11, GR^{villin}, con: n = 5–8, GR^{villin}, DSS: n = 3–7. All values are depicted as the mean ± SEM. Statistical analysis was performed by 1-way analysis of variance followed by Newman-Keuls Multiple Comparison test and is depicted for the comparison of GR^{flox} and GR^{villin} mice at each time point. Levels of significance: $^{*}P < .05$; $^{**}P < .01$; n.s., nonsignificant ($P > .5$).

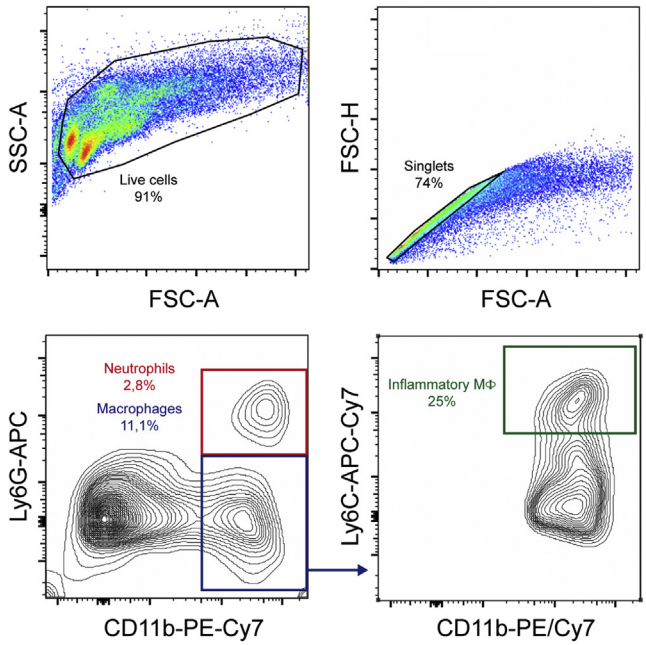

Figure 5. Gating strategy used for flow cytometric analysis of LPCs. Live cells were defined based on their forward and sideward scatter followed by gating on singlets. CD11b$^+$ myeloid cells (using a PE-Cy7-conjugated antibody) were subdivided into Ly6G$^+$ neutrophils and Ly6G$^-$ macrophages (using an APC-conjugated antibody). The inflammatory macrophage (MΦ) subpopulation was defined by further gating on Ly6C$^+$ cells among Ly6G$^-$ MΦ (using an APC-Cy7-conjugated antibody).

our laboratory revealed that GC effects on myeloid cells in the colon play an important role in the resolution phase of DSS-induced colitis, as the disease failed to resolve when the GR was absent in neutrophils and macrophages.[8] The role of the GR in IECs in the context of colitis, however, remained unclear. IECs fulfill a variety of crucial functions in the context of inflammatory diseases. They form a tight barrier against invading microorganisms from the lumen of the gut, are able to recognize bacteria by expressing pattern recognition receptors, and communicate this information to cells of the immune system by secreting chemoattractants. It is against this background that we hypothesized that GC activities in IECs play a crucial role in the pathogenesis of DSS-induced colitis. In fact, work published by others provided initial evidence that the GR in IECs influences inflammatory processes in the colon by showing that the deletion of the intestinal epithelial GR caused a transient upregulation of chemokines and cytokines in the gut.[17] However, no information was provided as to the involvement of the GR expressed in IECs under inflamed conditions.

In this work, we used the mouse model of DSS-induced colitis to further clarify the role of the GR in the colon. Importantly, our findings unveil a critical function of the intestinal epithelial GR in this disease and presumably UC as well. After selective GR ablation in IECs, DSS-induced colitis was aggravated. In contrast to the deletion of the GR in myeloid cells, the acute phase of the disease was affected rather than its resolution. GR^{villin} mice lost more weight than GR^{flox} mice, the clinical symptoms were aggravated, and the reduction in colon length was more pronounced. Furthermore, IL-6 serum levels as well as tissue damage in the colon and the concomitant loss of epithelial barrier integrity were enhanced in GR^{villin} compared with GR^{flox} mice. These findings indicate that the activity of endogenous GCs in IECs is instrumental in keeping DSS-induced colitis at bay.

Chemokines such as CXCL1 and CXCL5 are produced by IECs during colitis and serve to attract neutrophils and other immune cells.[25] Consequently, DSS-induced colitis was found to be aggravated in CXCL1-deficient mice, which was accompanied by a reduced neutrophil infiltration into the colon.[26] Intriguingly, gene expression of several chemokines including *Cxcl1* failed to be induced in IECs of GR^{villin} mice during DSS-induced colitis, which was associated with an exacerbated disease course and diminished neutrophil numbers in situ. This suggests that one mechanism by which GCs control colitis is the regulation of chemokine expression in IECs. While our data are in agreement with the supposed function of chemokines during colitis, they were unexpected from a mechanistic point of view, as GCs are mostly believed to suppress expression of inflammatory mediators.[27] Nevertheless, our observation is not unprecedented. In multiple sclerosis patients, for instance, it was shown that GCs increased T cell and monocyte migration along chemokine gradients.[28,29] It thus appears to be a common principle that GC promote chemoattraction during inflammation rather than diminishing it. From a physiological point of view, the reduced neutrophil infiltration into the colon of GR^{villin} mice should result in an impaired eradication of invading microorganisms, which could explain the aggravated DSS-induced colitis observed in mutant mice. We further suspect that the compromised clearance of pathogens in the colon accounts for the observed leukocyte hyperactivation, too, as revealed by the overexpression of several proinflammatory genes by LPCs.

GCs are also involved in the control of epithelial barrier integrity. Tumor necrosis factor α increases epithelial permeability during inflammation by binding to tumor necrosis factor receptor 2 (TNFR2) expressed on IECs and subsequently inducing MLCK (myosin light chain kinase), an effect that is counteracted by GCs.[30,31] TNF-α–induced barrier dysfunction also involves an upregulation of TNFR2, which is in line with the observation that TNFR2-deficient mice are protected from experimentally induced colitis.[31,32] The upregulation of *Tnfr2* and *Mlck* in IECs of GR^{villin} mice would therefore well explain the increased epithelial permeability in the colon.

Another central function of IECs is the recognition of harmful microorganisms in the gut lumen, which is achieved by expressing multiple pattern recognition receptors. TLR4 (Toll-like receptor 4) for instance is upregulated in IEC cell lines by proinflammatory cytokines[33] as well as in IECs of specimens collected from IBD patients.[34] These observations point toward an association between the severity of colitis and TLR4 expression in

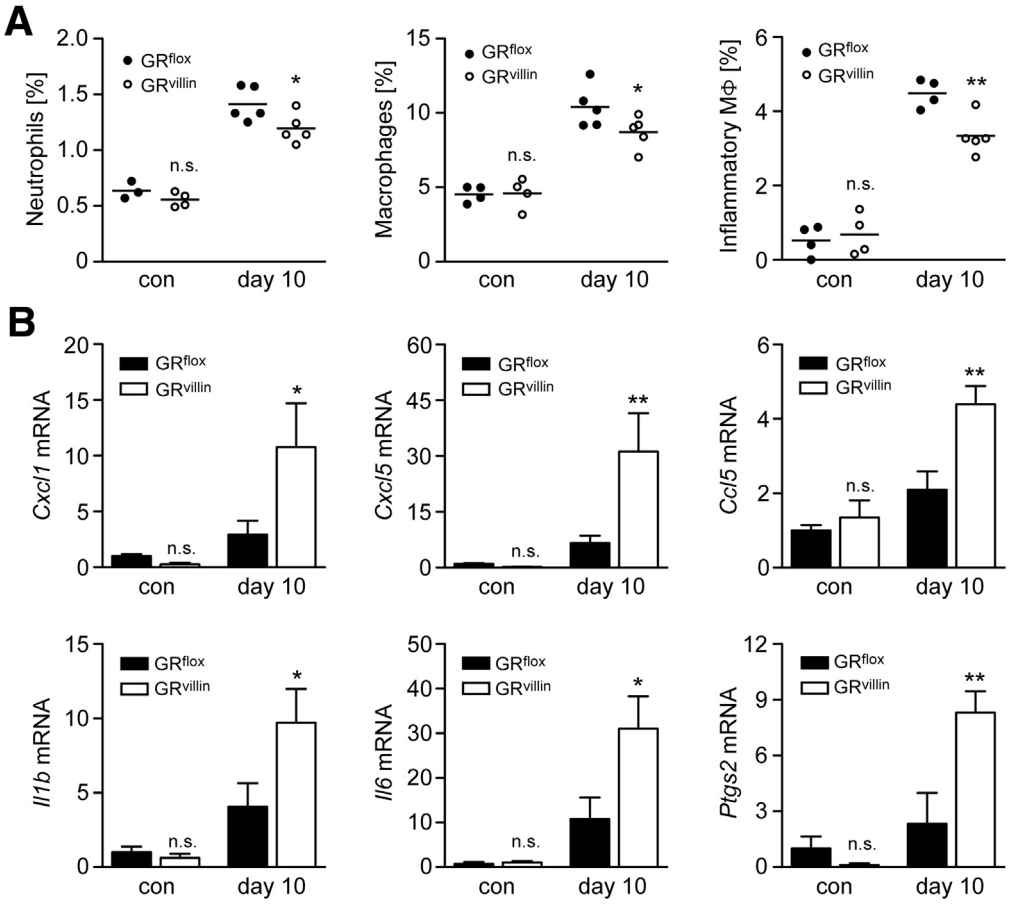

Figure 6. Leukocyte infiltration in the colon and gene expression in LPCs in DSS-induced colitis. GR^{flox} and GR^{villin} mice were treated with tamoxifen to initiate GR deletion in IECs and subsequently received DSS to induce colitis. Control (con) mice received only tap water. (*A*) LPCs were prepared by enzymatic digestion from the colon of DSS-treated mice at day 10 or control mice, and analyzed by flow cytometry. The percentages of neutrophils ($CD11b^{+}Ly6G^{+}$) and macrophages ($CD11b^{+}Ly6G^{-}$) among all LPCs, and the percentage of the inflammatory macrophage (MΦ) subpopulation ($Ly6C^{+}$) among $CD11b^{+}Ly6G^{-}$ macrophages are depicted as a dot plot, with each symbol corresponding to an individual mouse. GR^{flox}, con: n = 3–4, GR^{flox}, DSS: n = 4–5, GR^{villin}, con: n = 4, GR^{villin}, DSS: n = 5. (*B*) LPCs were prepared from the colon of DSS-treated mice at day 10 or control mice, followed by the analysis of gene expression by quantitative RT-PCR. Relative mRNA levels of *Cxcl1*, *Cxcl2*, and *Ccl5* as well as *Il1b*, *IL6*, and *Ptgs2* (*Cox2*) were determined by normalization to the housekeeping gene *Hprt*. Expression levels in untreated (con) GR^{flox} mice were arbitrarily set to 1. GR^{flox}, con: n = 4, GR^{flox}, DSS: n = 4–8, GR^{villin}, con: n = 4, GR^{villin}, DSS: n = 4–9. Values are depicted as the mean ± SEM. Statistical analysis was performed by 1-way analysis of variance followed by Newman-Keuls Multiple Comparison test and is depicted for the comparison of GR^{flox} and GR^{villin} mice at each time point. Levels of significance: $^{*}P < .05$; $^{**}P < .01$; n.s., nonsignificant ($P > .5$).

IECs similar to what we observed in GR^{villin} mice. We therefore propose that endogenous GCs repress *Tlr4* expression in IECs and thereby limit the activation of NF-κB signaling by invading bacteria. In the absence of the GR in IECs, *Tlr4* is overexpressed and thereby exaggerates inflammation in the colon.

UC is a risk factor for the development of CRC, which is mainly explained by the increased production of proinflammatory mediators. NF-κB signaling, IL-6 serum levels and COX-2 expression, for instance, were previously shown to contribute to tumorigenesis in the colon.[18,21,22,35] Increased gene expression of *Il1b*, *Il6*, and *Ptgs2 (Cox2)* in GR^{villin} mice thus can be expected to enhance tumor growth, although it is possible that the enhanced tissue damage contributes to an accumulation of gene mutations in IECs, too. Overall, our findings support the notion that there is a correlation between the severity of DSS-induced colitis, the underlying pathogenic events and the tumor burden in the AOM/DSS model. This conclusion is strengthened by our observation that the tumor burden was unaltered when deleting the GR after the acute phase of colitis, indicating that the severity of inflammation rather than the cell-intrinsic expression of the GR in IECs determines the strength of tumorigenesis.

Collectively, we provide evidence that endogenous GCs modulate the severity of colitis via their activity in IECs, which directly affects tumorigenesis in the colon. Hence, a better management of colitis by optimizing strategies of GC therapy could possibly reduce the risk of CA-CRC in human patients.

Materials and Methods

Animal Experimentation

GR^{flox} mice (*Nr3c1*^{tm2GSc}) and Villin-Cre^{ERT2} mice (*Tg(Vil1-cre/ERT2)23Syr*) on a C57BL/6 background have been described previously and were crossbred to generate GR^{villin} mice (*Nr3c1*^{tm2GSc}*;Tg(Vil1-cre/ERT2)23Syr*) as well as GR^{flox} littermate control mice.[36,37] All mice were kept in individually ventilated cages under specific pathogen–free conditions at the University Medical Center Göttingen, and only female mice were used at the age of 10–12 weeks. Animal experimentation was conducted according to international guidelines and approved by the responsible national authorities (*Nds. Landesamt für Verbraucherschutz und Lebensmittelsicherheit; Az: 33.9-42502-04-16/2075*).

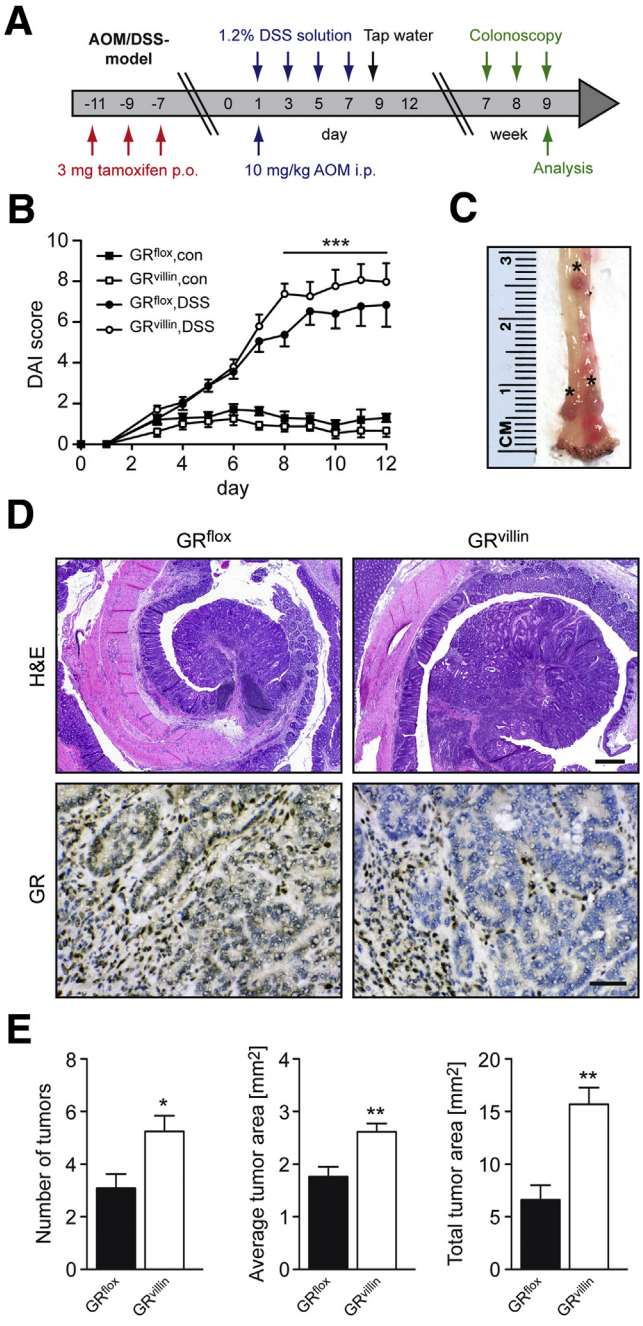

Figure 7. Impact of GR deletion in IECs on tumorigenesis in the AOM/DSS model. (*A*) Experimental setup of the AOM/DSS model. (*B*) GR^{flox} and GR^{villin} mice were treated as outlined in panel *A*. Control (con) mice received tap water instead of DSS. The DAI score was calculated based on stool consistence, intestinal bleeding and weight loss. GR^{flox} mice: n = 12/15, GR^{villin} mice: n = 12/17 (con/DSS). (*C*) DSS-treated mice of both genotypes were sacrificed in week 9 and macroscopically inspected for the presence of tumors. A representative photograph of a colon with tumors marked by asterisks, along with a ruler for size estimate, is depicted. (*D*) Swiss rolls were prepared from the colon of DSS-treated mice sacrificed in week 9. Paraffin sections were stained with hematoxylin and eosin or analyzed by immunohistochemistry after incubation with an anti-GR antibody. Representative photomicrographs acquired at 20× magnification are depicted for both genotypes. Scale bar = 500 μm (hematoxylin and eosin) or 75 μm (GR). (*E*) Tumors in the colon were enumerated and their size was measured using a caliper rule. The tumor area was calculated according to the formula $[(\text{length} + \text{width}) \times 0.5]^2$, and the total tumor area was obtained by multiplying tumor number and area for each mouse. GR^{flox} mice: n = 12, GR^{villin} mice: n = 12. Values are depicted as the mean ± SEM. Statistical analysis of panel *B* was performed by 1-way analysis of variance followed by Newman-Keuls Multiple Comparison test and is depicted for the comparison of GR^{flox} and GR^{villin} mice treated with DSS; data in panel E were analyzed by Mann-Whitney test. Levels of significance: $^*P < .05$; $^{**}P < .01$; $^{***}P < .001$; n.s., nonsignificant ($P > .5$).

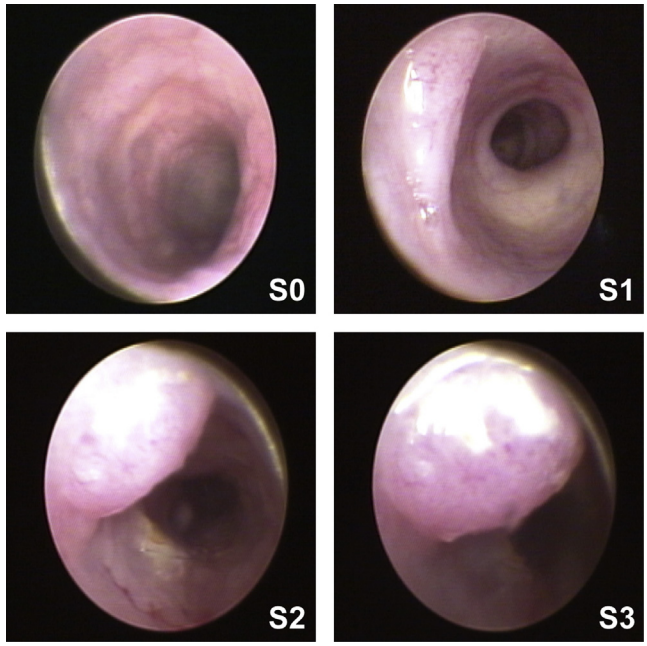

Figure 8. Monitoring tumorigenesis by colonoscopy. Representative photographs of stage S0 to S3 tumors in mice subjected to the AOM/DSS model of CA-CRC taken with the camera mounted to the colonoscope.

Recombination of the GR gene locus was induced by application of 9-mg tamoxifen in sunflower oil by oral gavage over a 5-day period. Successful recombination of the 2 loxP sites was confirmed as previously described.[38]

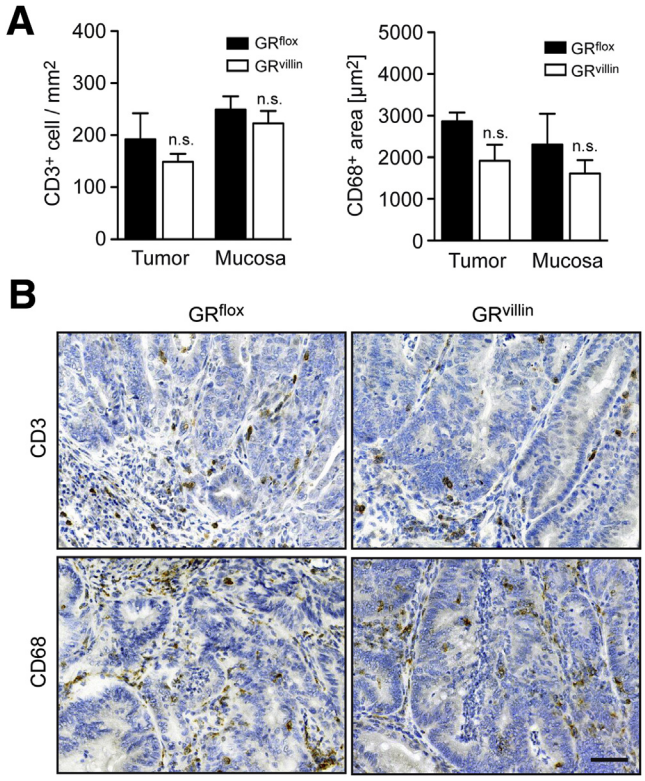

Figure 9. Leukocyte infiltration into the colon in the AOM/DSS model. GR^{flox} and GR^{villin} mice were treated with tamoxifen to initiate GR deletion. Thereafter, they were injected intraperitoneally with AOM at day 1 and additionally received DSS via the drinking water until day 8 as outlined in 7*A*. (*A*) DSS-treated mice of both genotypes were sacrificed in week 9 and paraffin sections were prepared from swiss rolls of the colon. Analysis was done by immunohistochemistry using either an anti-CD3 or anti-CD68 antibody. Computer-aided quantification of $CD3^+$ cells or the area occupied by $CD68^+$ cells was separately performed for the tumor as well as for neighboring mucosa. Statistical analysis was performed by 1-way analysis of variance followed by Newman-Keuls Multiple Comparison test. (*B*) Representative photomicrographs of tissue sections corresponding to the center of the tumor and acquired at 20× magnification. Scale bar = 75 μm. n.s., nonsignificant ($P > .5$).

Mouse Model of DSS-Induced Colitis

Disease induction was essentially performed as previously described[8] using DSS at a concentration of 1.2%. Control mice received tap water only. The severity of DSS-induced colitis was assessed based on body weight, DAI, and colon length, as described previously.[8]

Mouse Model of AOM/DSS-Induced Tumorigenesis

Disease induction was performed by injecting the mice with 10-mg/kg AOM intraperitoneally immediately followed by the treatment with DSS for 8 days.[39] Clinical symptoms of DSS-induced colitis were evaluated until day 12, as outlined previously, and tumor development was monitored by colonoscopy from week 7 to 9 (Figure 8).

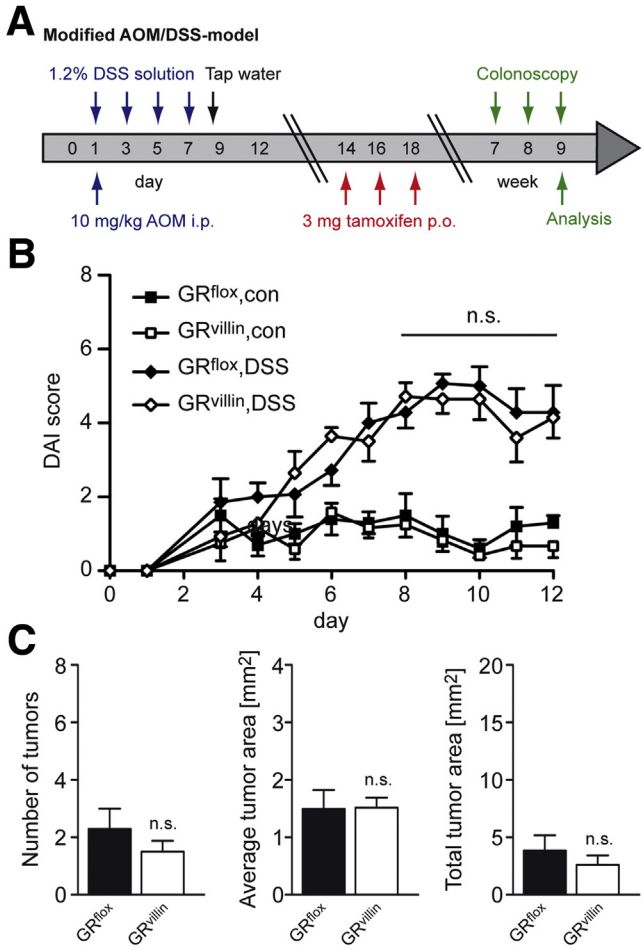

Figure 10. Differential impact of inflammation and GR deletion on tumorigenesis in the AOM/DSS model. (*A*) Experimental setup of the modified AOM/DSS model. (*B*) GR^{flox} and GR^{villin} mice were treated as outlined in panel *A*. Control (con) mice received tap water only. Mice of all groups were injected intraperitoneally with AOM at day 1. The DAI score was calculated based on stool consistence, intestinal bleeding and weight loss. GR^{flox} mice: n = 6/7 (con/DSS), GR^{villin} mice: n = 5/8 (con/DSS). (*C*) At the end of the acute phase of DSS-induced colitis, GR deletion was initiated by tamoxifen treatment starting at day 14. Mice were sacrificed in week 9, tumors in the colon were enumerated and their size measured using a caliper rule. The tumor area was calculated according to the formula $[(\text{length} + \text{width}) \times 0.5]^2$, and the total tumor area was obtained by multiplying tumor number and area for each mouse. GR^{flox} mice: n = 7, GR^{villin} mice: n = 8. Values are depicted as the mean ± SEM. Statistical analysis of panel *B* was performed by 1-way analysis of variance followed by Newman-Keuls Multiple Comparison test and is depicted for the comparison of GR^{flox} and GR^{villin} mice treated with DSS; data in panel *C* were analyzed by Mann-Whitney test. n.s., nonsignificant ($P > .5$).

Assessment of the Intestinal Epithelial Barrier Integrity

An EB assay was performed to determine the permeability of the intestinal epithelium.[40] To this end, the colon was removed and flushed with ice-cold phosphate-buffered

Table 1. Primer Sequences

Gene	Forward Primer	Reverse Primer
Actb	AGCCATGTACGTAGCCATCC	CTCTCAGCTGTGGTGGTGAA
Ccl2	GACCTTAGGGCAGATGCAGT	AGCTGTAGTTTTTGTCACCAAGC
Ccl3	TCAGGAAAATGACACCTGGCTG	ATATGGAGCTGACACCCCGA
Ccl5	CGACTGCAAGATTGGAGCAC	CTCACCATATGGCTCGGACA
Ccl7	CTCGACCCACTTCTGATGGG	CCCTGGGAAGCTGTTATCTTCAA
Cx3cr1	TCGCCCAAATAACAGGCC	TGTCCACCTCCTTCCCTGAA
Cxcl1	CTCCGTTACTTGGGGACACC	ACCGAAGTCATAGCCACACTC
Cxcl2	CAGGTACGATCCAGGCTTCC	TGAACAAAGGCAAGGCTAACTG
Cxcl5	AGCTTTCTTTTTGTCACTGCCC	TGCCCTACGGTGGAAGTCAT
Hprt	GGGACGCAGCAACTGACATT	GTCCTGTGGCCATCTGCCTA
Il1b	AAGCAGCCCTTCATCTTTTG	CTCATCTGGGATCCTCTCCA
Il6	CAGAATTGCCATTGCACAAC	AGTTGCCTTCTTGGGACTGA
Mlck	CTCCTTGTTCTCCTCCGGGC	TTCCAGAATTCCAAGGTGGCTG
Oct	TGCTGCAAAATTCGGGATGC	TGCTGCAAAATTCGGGATGC
Ptgs2	GATACACCTCTCCACCAATGACC	CAGACAACATAAACTGCGCCTT
Rna18s	CCATCCAATCGGTAGTAGCG	GTAACCCGTTGAACCCCATT
Tlr2	CATCCTCTGAGATTTGACGCTTT	CTGGAGCATCCGAATTGCA
Tlr4	TAGGAACTACCTCTATGCAGGG	TGGTTGCAGAAAATGCCAGG
Tnfr2	TGGGTTTTCAAGGCGGCAGTA	ACCACTGACCAGGTGGAGAT

saline (PBS). The rectum was closed, instilled with 0.3 mL of 0.02% EB solution in PBS before closing the oral end of the colon. The so prepared bowel sac was then incubated on ice for 1 hour and subsequently washed with 0.1 M acetylcysteine. Finally, it was dried at 37°C overnight and weighed. To extract the dye from the colonic tissue, it was cut into small pieces and incubated in 1-mL formamide at 56°C for 24 hours. After centrifugation, the absorption of the supernatant was measured at a wavelength of 620 nm, and the concentration of the extracted EB was calculated with the help of a standard curve.

Enzyme-Linked Immunosorbent Assay

Serum was prepared from blood samples collected by cardiac puncture and the level of IL-6 was measured by enzyme-linked immunosorbent assay using a commercially available kit according to the manufacturer's instructions (BioLegend, Uithoorn, the Netherlands).

Histology

Swiss rolls from the colon were prepared as described previously.[8] Histopathological evaluation of the entire section corresponding to the full length of the colon was performed in a blinded manner as described previously.[8]

Immunohistochemistry

Tissue sections were incubated in EnVision Flex Target Retrival Solution (Dako, Santa Clara, CA) followed by incubation with an antibody recognizing the GR (1:200; M20; Santa Cruz Biotechnology, Heidelberg, Germany), CD3 (1:2000; Santa Cruz Biotechnology), or CD68 (1:200; Abcam, Cambridge, United Kingdom) for 30 minutes.[41] A polymeric secondary antibody coupled to horseradish peroxidase (ImmPRESS HRP Polymer Detection Kit; Vector Laboratories, Burlingame, CA) and DAB (Dako) were used to visualize immunoreactivity (dark brown staining). Hematoxylin was used for counterstaining and photomicrographs were acquired with an Olympus VS120 Virtual Slide Microscope (Olympus, Hamburg, Germany). Enumeration of $CD3^+$ T cells and quantification of the area covered by $CD68^+$ macrophages was performed by using ImageJ software (version 1.52n; National Institutes of Health, Bethesda, MD).

Isolation of IECs and LPCs

The different cell populations from colonic tissue were isolated as described previously.[42] In short, the colon was opened, washed, and transferred into a tube filled with PBS, and the IECs were isolated by vigorous shaking. LPCs were isolated by adding 100-U/mL collagenase 1A, 100-U/mL collagenase II, and 50-U/mL DNase II (all from Sigma-Aldrich, St Louis, MO) in RPMI/10% fetal calf serum (Thermo Fisher Scientific, Waltham, MA) and incubated at 37°C for 30 minutes while repeatedly vortexing. The LPC suspension was passed through a 40-μm cell strainer and finally washed with PBS.

Quantitative RT-PCR

Total RNA from IECs and LPCs was isolated using the Quick-RNA MiniPrep kit (Zymo Research, Irvine, CA) followed by purification of mRNA with the Dynabeads mRNA DIRECT kit (Thermo Fisher Scientific). Total RNA from colon

tissue was isolated with the help of the RNeasy Mini kit (Qiagen, Hilden, Germany). Reverse transcription into complementary DNA was achieved with the iScript kit (Bio-Rad, Munich, Germany), and quantitative RT-PCR was performed on an ABI 7500 instrument (Applied Biosystems, Darmstadt, Germany) using the SYBR green Master Mix from the same company. The following protocol was employed for DNA amplification: step 1 (2 minutes, 50°C), step 2 (10 minutes, 95°C), step 3 (15 seconds, 95°C; 1 minute, 60 °C; 40 cycles), step 4 (dissociation, melting curve). The housekeeping gene *Hprt* was used for normalization, and relative levels of gene expression were calculated with the ΔΔCt method after testing the assay for geometric efficacy. Notably, mRNA levels of *Hprt* were proportional to mRNA levels of the housekeeping genes *Rna18s* and *Actb* as determined by linear regression analysis. All oligonucleotides were synthesized by Metabion (Munich, Germany), primer sequences are listed in Table 1.

Fluidigm Gene Chip Analysis

Gene expression analysis by high-throughput quantitative PCR was performed using 48.48 Dynamic Arrays (Fluidigm, San Francisco, CA) and the BioMark HD system as described.[42] BioMark Data Collection software (Fluidigm) was employed for quantitative RT-PCR and melting curve analysis. Gene expression was normalized to the housekeeping gene *Hprt*, and relative expression levels were calculated by using the ΔΔCt method.

Flow Cytometry

In order to analyze LPCs, an FcR blockade was initially performed by incubation with TruStain fcX (anti-mouse CD16/32; clone: 93) followed by staining the cells with a cocktail of monoclonal antibodies containing anti-CD11b (clone: M1/70), anti-Ly6G (clone: 1A8), and anti-Ly6C (clone: HK1.4). The gating strategy is illustrated in Figure 5. To determine the purity of IEC preparations, which was routinely found to be >80%, the cells were stained with an anti-CD326 monoclonal antibody or rat IgG2a as an isotype control. Data were acquired on a FACS (fluorescence activated cell sorting) Canto II device (BD Bioscience) and analyzed using FlowJo software (version v10; Tree Star, Ashland, OR). All antibodies were purchased from BioLegend.

Statistical analysis

The data were analyzed using GraphPad Prism software (version 8; GraphPad Software, San Diego, CA) and are depicted as mean values ± SEM. One-way analysis of variance followed by Newman-Keuls Multiple Comparison test or Mann Whitney test were used for statistical analysis. Levels of significance: $*P < .05$; $**P < .01$; $***P < .001$; nonsignificant, $P > .05$.

Data access

All authors had access to the study data and reviewed and approved the final manuscript.

References

1. Baumgart DC, Sandborn WJ. Inflammatory bowel disease: clinical aspects and established and evolving therapies. Lancet 2007;369:1641–1657.
2. Danese S, Fiocchi C. Ulcerative colitis. N Engl J Med 2011;365:1713–1725.
3. Wânderas MH, Moum BA, Høvik ML, Høvde Ø. Predictive factors for a severe clinical course in ulcerative colitis: Results from population-based studies. World J Gastrointest Pharmacol Ther 2016;7:235–241.
4. Yashiro M. Ulcerative colitis-associated colorectal cancer. World J Gastroenterol 2014;20:16389–16397.
5. Pithadia AB, Jain S. Treatment of inflammatory bowel disease (IBD). Pharmacol Rep 2011;63:629–642.
6. Khan HM, Mehmood F, Khan N. Optimal management of steroid-dependent ulcerative colitis. Clin Exp Gastroenterol 2015;8:293–302.
7. Schäcke H, Döcke WD, Asadullah K. Mechanisms involved in the side effects of glucocorticoids. Pharmacol Ther 2002;96:23–43.
8. Meers GK, Bohnenberger H, Reichardt HM, Lühder F, Reichardt SD. Impaired resolution of DSS-induced colitis in mice lacking the glucocorticoid receptor in myeloid cells. PLoS One 2018;13:e0190846.
9. Crielaard BJ, Lammers T, Morgan ME, Chaabane L, Carboni S, Greco B, Zaratin P, Kraneveld AD, Storm G. Macrophages and liposomes in inflammatory disease: friends or foes? Int J Pharm 2011;416:499–506.
10. Kojouharoff G, Hans W, Obermeier F, Mannel DN, Andus T, Scholmerich J, Gross V, Falk W. Neutralization of tumour necrosis factor (TNF) but not of IL-1 reduces inflammation in chronic dextran sulphate sodium-induced colitis in mice. Clin Exp Immunol 1997;107:353–358.
11. Zhang Z, Dong L, Jia A, Chen X, Yang Q, Wang Y, Wang Y, Liu R, Cao Y, He Y, Bi Y, Liu G. Glucocorticoids promote the onset of acute experimental colitis and cancer by upregulating mTOR signaling in intestinal epithelial cells. Cancers (Basel) 2020;12:945.
12. Kagnoff MF. The intestinal epithelium is an integral component of a communications network. J Clin Invest 2014;124:2841–2843.
13. Abreu MT. Toll-like receptor signalling in the intestinal epithelium: how bacterial recognition shapes intestinal function. Nat Rev Immunol 2010;10:131–144.
14. Odenwald MA, Turner JR. The intestinal epithelial barrier: a therapeutic target? Nat Rev Gastroenterol Hepatol 2017;14:9–21.
15. Prasad S, Mingrino R, Kaukinen K, Hayes KL, Powell RM, MacDonald TT, Collins JE. Inflammatory processes have differential effects on claudins 2, 3 and 4 in colonic epithelial cells. Lab Invest 2005;85:1139–1162.
16. Schmitz H, Barmeyer C, Fromm M, Runkel N, Foss HD, Bentzel CJ, Riecken EO, Schulzke JD. Altered tight junction structure contributes to the impaired epithelial barrier function in ulcerative colitis. Gastroenterology 1999;116:301–309.
17. Aranda CJ, Arredondo-Amador M, Ocon B, Lavin JL, Aransay AM, Martinez-Augustin O, Sanchez de Medina F. Intestinal epithelial deletion of the

glucocorticoid receptor NR3C1 alters expression of inflammatory mediators and barrier function. FASEB J 2019;33:14067–14082.
18. Hirano T, Hirayama D, Wagatsuma K, Yamakawa T, Yokoyama Y, Nakase H. Immunological mechanisms in inflammation-associated colon carcinogenesis. Int J Mol Sci 2020;21:3062.
19. Karin M. Nuclear factor-kappaB in cancer development and progression. Nature 2006;441:431–436.
20. Greten FR, Eckmann L, Greten TF, Park JM, Li ZW, Egan LJ, Kagnoff MF, Karin M. IKKbeta links inflammation and tumorigenesis in a mouse model of colitis-associated cancer. Cell 2004;118:285–296.
21. Knüpfer H, Preiss R. Serum interleukin-6 levels in colorectal cancer patients–a summary of published results. Int J Colorectal Dis 2010;25:135–140.
22. Oshima M, Dinchuk JE, Kargman SL, Oshima H, Hancock B, Kwong E, Trzaskos JM, Evans JF, Taketo MM. Suppression of intestinal polyposis in Apc delta716 knockout mice by inhibition of cyclooxygenase 2 (COX-2). Cell 1996;87:803–809.
23. Zhao R, Coker OO, Wu J, Zhou Y, Zhao L, Nakatsu G, Bian X, Wei H, Chan AWH, Sung JJY, Chan FKL, El-Omar E, Yu J. Aspirin reduces colorectal tumor development in mice and gut microbes reduce its bioavailability and chemopreventive effects. Gastroenterology 2020;159:969–983.e4.
24. Grancher A, Michel P, Di Fiore F, Sefrioui D. [Aspirin and colorectal cancer]. Bull Cancer 2018;105:171–180.
25. Kulkarni N, Pathak M, Lal G. Role of chemokine receptors and intestinal epithelial cells in the mucosal inflammation and tolerance. J Leukoc Biol 2017;101:377–394.
26. Shea-Donohue T, Thomas K, Cody MJ, Aiping Z, Detolla LJ, Kopydlowski KM, Fukata M, Lira SA, Vogel SN. Mice deficient in the CXCR2 ligand, CXCL1 (KC/GRO-alpha), exhibit increased susceptibility to dextran sodium sulfate (DSS)-induced colitis. Innate Immun 2008;14:117–124.
27. Escoter-Torres L, Caratti G, Mechtidou A, Tuckermann J, Uhlenhaut NH, Vettorazzi S. Fighting the fire: mechanisms of inflammatory gene regulation by the glucocorticoid receptor. Front Immunol 2019;10:1859.
28. Fischer HJ, Finck TLK, Pellkofer HL, Reichardt HM, Lühder F. Glucocorticoid therapy of multiple sclerosis patients induces anti-inflammatory polarization and increased chemotaxis of monocytes. Front Immunol 2019;10:1200.
29. Schweingruber N, Reichardt SD, Lühder F, Reichardt HM. Mechanisms of glucocorticoids in the control of neuroinflammation. J Neuroendocrinol 2012;24:174–182.
30. Boivin MA, Ye D, Kennedy JC, Al-Sadi R, Shepela C, Ma TY. Mechanism of glucocorticoid regulation of the intestinal tight junction barrier. Am J Physiol Gastrointest Liver Physiol 2007;292:G590–G598.
31. Wang F, Schwarz BT, Graham WV, Wang Y, Su L, Clayburgh DR, Abraham C, Turner JR. IFN-gamma-induced TNFR2 expression is required for TNF-dependent intestinal epithelial barrier dysfunction. Gastroenterology 2006;131:1153–1163.
32. Ebach DR, Newberry R, Stenson WF. Differential role of tumor necrosis factor receptors in TNBS colitis. Inflamm Bowel Dis 2005;11:533–540.
33. Abreu MT, Arnold ET, Thomas LS, Gonsky R, Zhou Y, Hu B, Arditi M. TLR4 and MD-2 expression is regulated by immune-mediated signals in human intestinal epithelial cells. J Biol Chem 2002;277:20431–20437.
34. Cario E, Podolsky DK. Differential alteration in intestinal epithelial cell expression of toll-like receptor 3 (TLR3) and TLR4 in inflammatory bowel disease. Infect Immun 2000;68:7010–7017.
35. Heinsbroek SE, Gordon S. The role of macrophages in inflammatory bowel diseases. Expert Rev Mol Med 2009;11:e14.
36. el Marjou F, Janssen KP, Chang BH, Li M, Hindie V, Chan L, Louvard D, Chambon P, Metzger D, Robine S. Tissue-specific and inducible Cre-mediated recombination in the gut epithelium. Genesis 2004;39:186–193.
37. Tronche F, Kellendonk C, Kretz O, Gass P, Anlag K, Orban PC, Bock R, Klein R, Schütz G. Disruption of the glucocorticoid receptor gene in the nervous system results in reduced anxiety. Nat Genet 1999;23:99–103.
38. Reichardt SD, Föller M, Rexhepaj R, Pathare G, Minnich K, Tuckermann JP, Lang F, Reichardt HM. Glucocorticoids enhance intestinal glucose uptake via the dimerized glucocorticoid receptor in enterocytes. Endocrinology 2012;153:1783–1794.
39. Wirtz S, Neufert C, Weigmann B, Neurath MF. Chemically induced mouse models of intestinal inflammation. Nat Protoc 2007;2:541–546.
40. Ding H, Mei Q, Gan HZ, Cao LY, Liu XC, Xu JM. Effect of homocysteine on intestinal permeability in rats with experimental colitis, and its mechanism. Gastroenterol Rep (Oxf) 2014;2:215–220.
41. Klaßen C, Karabinskaya A, Dejager L, Vettorazzi S, Van Moorleghem J, Lühder F, Meijsing SH, Tuckermann JP, Bohnenberger H, Libert C, Reichardt HM. Airway epithelial cells are crucial targets of glucocorticoids in a mouse model of allergic asthma. J Immunol 2017;199:48–61.
42. Li H, Kaiser TK, Borschiwer M, Bohnenberger H, Reichardt SD, Lühder F, Walter L, Dressel R, Meijsing SH, Reichardt HM. Glucocorticoid resistance of allogeneic T cells alters the gene expression profile in the inflamed small intestine of mice suffering from acute graft-versus-host disease. J Steroid Biochem Mol Biol 2019;195:105485.

Received November 2, 2020. Accepted December 7, 2020.

Correspondence
Address correspondence to: Sybille Reichardt, PhD, Institute for Cellular and Molecular Immunology, University Medical Center Göttingen, Humboldtallee 34, 37073 Göttingen, Germany. e-mail: sybille.reichardt@med.uni-goettingen.de; fax: +49 551-395843.

Acknowledgments
The authors thank Amina Bassibas and Jennifer Appelhans for expert technical assistance and Cathy Ludwig for language editing.

CRediT Authorship Contributions
Chiara Muzzi, MSc (Data curation: Lead; Formal analysis: Lead)
Norika Watanabe, student (Data curation: Equal; Formal analysis: Equal)
Eric Twomey, student (Data curation: Equal; Formal analysis: Equal)
Garrit K. Meers, student (Data curation: Supporting; Formal analysis: Supporting)
Holger M. Reichardt, PhD (Formal analysis: Supporting; Writing – original draft: Equal; Writing – review & editing: Equal)
Hanibal Bohnenberger, MD (Methodology: Supporting; Resources: Supporting; Writing – review & editing: Supporting)
Sybille Reichardt, PhD (Conceptualization: Lead; Formal analysis: Lead; Funding acquisition: Lead; Writing – original draft: Lead)

Conflicts of Interest
The authors disclose no conflicts.

Funding
This work was supported by grants from Deutsche Forschungsgemeinschaft (RE 4439/1-1) and intramural funds of the University Medical Center Göttingen (Heidenreich von Siebold Program), both to S.D.R. We acknowledge support by the Open Access Publication Funds of the Göttingen University